Vibrational Absorption and Circular Dichroism Studies of (−)-Camphanic Acid

Thierry Buffeteau,*,† Dominique Cavagnat,† Aude Bouchet,† and Thierry Brotin‡

Laboratoire de Physico-Chimie Moléculaire, UMR 5803 du CNRS, Université Bordeaux I, 351 Cours de la Libération, 33405 Talence, France, and Laboratoire de Chimie de l'ENS-LYON, UMR 5182 du CNRS, Ecole Normale Supérieure de Lyon, 46 Allée d'Italie, 69364 Lyon 07, France

Received: September 29, 2006; In Final Form: November 20, 2006

Vibrational absorption and circular dichroism (VCD) spectra of (−)-(1*S*,3*R*)-camphanic acid have been measured in deuterated chloroform solutions at different concentrations (0.005, 0.045, and 0.200 M) in the mid-infrared spectral range. Experimental spectra have been compared with the density functional theory (DFT) absorption and VCD spectra, calculated using the B3PW91 functional and cc-pVTZ basis set for three conformers of both the monomer and the dimer forms of (−)-(1*S*,3*R*)-camphanic acid. These calculations indicate that, in the dilute solution, the conformer with intramolecular hydrogen-bonding between the hydroxyl and lactone groups is of lowest energy and represents 70% of the different monomer conformers at room temperature, whereas, in concentrated solution, the dimer formed by intermolecular hydrogen-bonding of carboxyl groups of the two distinct monomer conformations is stabilized. The vibrational absorption and circular dichroism spectra calculated from the Boltzmann population of the individual monomer and dimer conformers are in very good overall agreement with the corresponding experimental spectra, allowing the absolute conformation and configuration of (−)-(1*S*,3*R*)-camphanic acid in dilute and concentrated solution, respectively. Experiments were also performed on (−)-(1*S*,3*R*)-camphanic chloride for which the populations predicted by DFT calculations are found to be in disagreement with those deduced from experimental spectra.

1. Introduction

Vibrational circular dichroism (VCD) is the differential absorption by chiral molecules of left- and right-handed circularly polarized radiation in the infrared (IR) region.[1] During the past decade, VCD appeared as a very promising tool for the study of the conformational analysis of chiral organic compounds.[2] Indeed, the VCD spectrum of a chiral molecule is very dependent on its absolute configuration, and in the case of flexible molecules on its conformation. The relation between the VCD spectrum and the structure of a chiral molecule can be rationalized from quantum mechanical calculations.[3] By comparing the experimental spectrum with the calculated spectrum of one enantiomer with a given conformation, it is possible to identify the absolute configuration and the conformation of a chiral molecule.

(1*S*,3*R*)-Camphanic acid (lactone of 1-hydroxy-2,2,3-trimethylcyclopentan-1,3-dicarboxylic acid), **1**, and (1*S*,3*R*)-camphanic chloride, **2**, are well-known chiral auxiliary agents used for separation of racemates.[4−6] Even though these compounds are repeatedly used, there is no literature report on the stereochemistry of these chiral molecules. The monomer of **1** and **2** can assume two conformations that differ by 180° rotation of the COOH and COCl groups, labeled **1a**, **1b** and **2a**, **2b**, respectively, in Chart 1. For the camphanic acid, a third conformation (labeled **1c**) with intramolecular hydrogen-bonding between the hydroxyl and lactone groups is also possible. Moreover, when the solution concentration increases, carboxylic acid dimer formation occurs (intermolecular hydrogen-bonding between two carboxylic acid groups), giving rise to three dimer conformers **1aa**, **1bb**, and **1ab**, as shown in Chart 1. Consequently, the determination of the absolute conformation of carboxylic acids is not trivial because the monomeric and dimeric forms coexist in solution for usual concentration. Besides the academic interest to investigate the dimer formation and the molecular stereochemistry of chiral carboxylic acids by VCD, this work has particular relevance to studies of the absolute conformation of pharmaceutical molecules as many have acid groups.

A few examples reported in the literature have demonstrated the sensitivity of the VCD to carboxylic acid dimer formation.[2,7,8] Freedman et al.[2] showed for (*S*)-2-phenyl-propionic acid that dramatic changes are predicted in both IR and VCD spectra in going from the monomer to dimer and that the dimer is the most abundant species in a 0.18 M $CDCl_3$ solution. More recently, He et al.[7] revealed that the predicted IR and VCD spectra for the monomer conformation of α-aryloxylpropanoic acids did not reproduce the corresponding experimental spectra. On the other hand, the population-weighted IR and VCD spectra for dimeric acids were found to be in good agreement with the corresponding spectra in $CDCl_3$ solution. Finally, Urbanova et al.[8] showed that oligomerization of (*S*)-2,2′-dimethyl-biphenyl-6,6′-dicarboxylic acid occurred in $CDCl_3$ solution with increasing concentration. VCD and density functional theory (DFT) calculations supported the conclusion that the oligomer formed was the cyclic tetramer in which monomers were linked by intermolecular hydrogen-bonding between two COOH groups. In these three studies, the dimeric form has been observed because experiments were performed at concentration greater than 0.15 M and using a limited path length cell. These experimental conditions have been chosen to increase the signal-to-noise ratio (S/B) of the VCD spectra and to limit interference with the solvent ($CDCl_3$) absorptions.

* Corresponding author. Fax: (33) 5 40 00 84 02. E-mail: t.buffeteau@lpcm.u-bordeaux1.fr.

† Université Bordeaux I.

‡ Ecole Normale Supérieure de Lyon.

10.1021/jp066402w CCC: $37.00
Published on Web 01/24/2007

CHART 1:

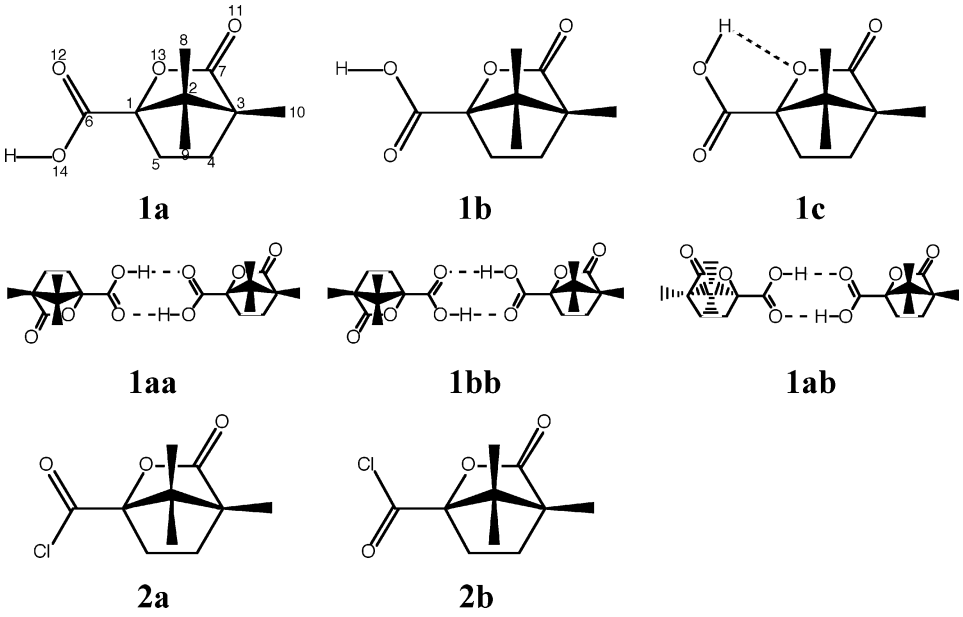

The main objective of this article was to determine the predominant conformations of (1*S*,3*R*)-camphanic acid for its monomeric and dimeric forms. To obtain the monomer of **1**, experiments were performed for a dilute (0.005 M) $CDCl_3$ solution. The measurement of the VCD spectrum at this concentration and using a path length of 475 μm (interference with solvent absorption occurs for higher path length) presented a challenge, as the absorption of the compound did not exceed 0.03. Experiments were also performed for a more concentrated (0.200 M) solution to favor the dimeric form of **1**, as well as at an intermediate (0.045 M) concentration to obtain the VCD spectra with a sufficient S/B in the spectral range associated with OH and CH stretching vibrations. Finally, to eliminate the influence of inter- and intramolecular hydrogen-bonding effects, (1*S*,3*R*)-camphanic chloride has been subjected to experimental and theoretical VCD investigations. The calculations of the IR and VCD intensities of **1** for its monomeric and dimeric forms and of **2** have been made at the DFT level using the B3PW91 functional and cc-pVTZ basis set.

2. Experimental Section

Materials. (−)-(1*S*,3*R*)-Camphanic acid, **1**, and (−)-(1*S*,3*R*)-camphanic chloride, **2**, were obtained from Sigma and studied without further purification in $CDCl_3$ solutions. To prevent formation of camphanic acid, **2** was dissolved in anhydrous $CDCl_3$.

FTIR Measurements. The infrared and VCD spectra were recorded with a ThermoNicolet Nexus 670 FTIR spectrometer equipped with a VCD optical bench.[9] In this optical bench, the light beam was focused on the sample by a BaF_2 lens (191 mm focal length), passing an optical filter (depending on the studied spectral range), a BaF_2 wire grid polarizer (Specac), and a ZnSe photoelastic modulator (Hinds Instruments, Type II/ZS50). The light was then focused by a ZnSe lens (38.1 mm focal length) onto a 1 × 1 mm^2 HgCdTe (ThermoNicolet, MCTA* E6032) detector. Absorption and VCD spectra were recorded at a resolution of 4 cm^{-1}, by coadding 50 scans and 24 000 scans (8 h acquisition time), respectively. Samples were held in a variable path length cell with BaF_2 windows. Spectra of **1** were measured in $CDCl_3$ solvent at three concentrations, 0.005 M (path length of 475 μm), 0.045 M (path length of 915 μm for OH/CH stretching region and 165 μm for mid-IR spectral region), and 0.200 M (path length of 95 μm). Spectra of **2** were measured in $CDCl_3$ solvent at a concentration of 0.050 M and at a path length of 240 μm. Baseline corrections of the VCD spectra were performed by subtracting the raw VCD spectra of the solvent. The photoelastic modulator was adjusted for a maximum efficiency at 1400 and 3200 cm^{-1} for experiments in the mid-IR and OH/CH stretching regions, respectively. Calculations were performed via the standard ThermoNicolet software, using Happ and Genzel apodization, de-Haseth phase-correction, and a zero-filling factor of 1. Calibration spectra were recorded using a birefringent plate (CdSe) and a second BaF_2 wire grid polarizer, following the experimental procedure previously published.[10] Finally, in the presented absorption spectra, the solvent absorption was subtracted out.

Theoretical Calculations. The geometry optimizations, vibrational frequencies, and absorption and VCD intensities were calculated by the Gaussian 03 program[11] on four processors on a SGI ALTIX3300. Calculations of the optimized geometry of **1a**, **1b**, **1c**, **1aa**, **1bb**, **1ab**, **2a**, and **2b** conformers were performed at the density functional theory level using the B3PW91 functional and cc-pVTZ basis set. Vibrational frequencies and IR and VCD intensities were calculated at the same level of theory, utilizing the magnetic field perturbation method with gauge-invariant atomic orbitals.[12] For comparison to experiment, the calculated frequencies were scaled by 0.978 (0.954), and the calculated intensities were converted to Lorentzian bands with a half-width of 7 cm^{-1} for the 1850−950 cm^{-1} (3600−2700 cm^{-1}) spectral range. All of the calculations were performed for the isolated molecule.

3. Results and Discussion

Experimental IR and VCD Spectra of 1 and 2. The concentration dependence of the IR spectrum of **1** in $CDCl_3$ solution in the OH/CH stretching region and in the mid-IR spectral region is shown in Figure 1a and b, respectively. The observation of the concentration-dependent IR spectrum in the OH/CH stretching region demonstrates that dimerization of **1** occurs in $CDCl_3$ solvent with increasing concentration. Dimerization of carboxylic acids in nonpolar solvents via intermolecular hydrogen-bonding is well-known and can be easily

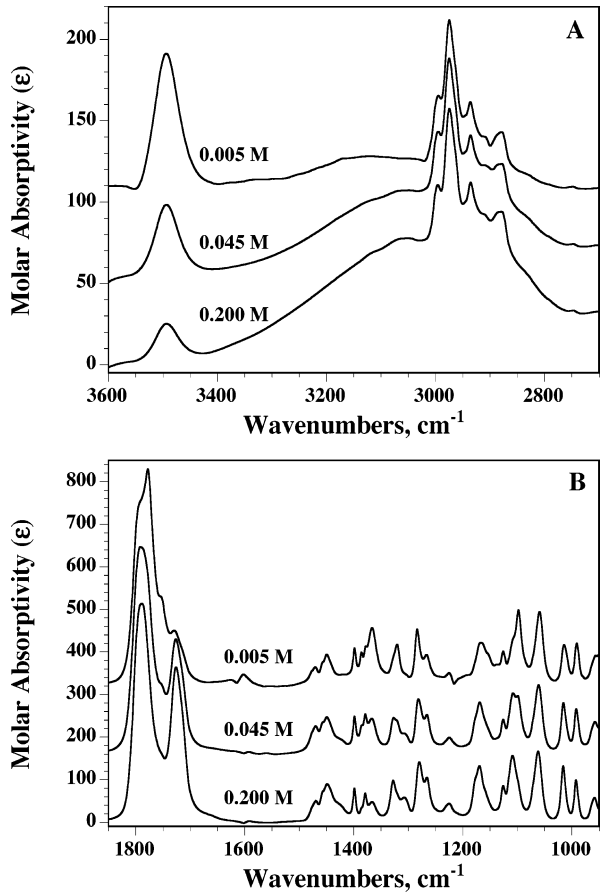

Figure 1. Concentration dependence of the IR spectra of **1** in $CDCl_3$ solution (A) in the OH/CH stretching region and (B) in the mid-IR spectral region.

followed from the OH stretching vibration of the carboxylic groups. Indeed, the monomeric form of **1** contains "free" (i.e., non-hydrogen-bonded) COOH groups, which are expected to give rise to OH stretching vibration at high wavenumbers (close to 3500 cm^{-1}). The dimeric form of **1**, forming $(COOH)_2$ moieties, is expected to subtantially decrease the OH stretching frequencies.[13] Consequently, formation of dimers should be accompanied in the IR spectra by a decrease in intensity of the OH stretching vibration of "free" COOH groups and the appearance of a new band at lower wavenumbers, associated with OH stretching vibration of hydrogen-bonded COOH groups. This expected pattern is observed in Figure 1a. A band at 3494 cm^{-1} is observed for the 0.005 M $CDCl_3$ solution of **1**, which decreases in intensity with increasing concentration. This band is assigned to the OH stretching vibration of "free" COOH groups. Its disappearance with increasing concentration coupled with the appearance of a broad band near 3000 cm^{-1} is consistent with the formation of dimers. As this broad band is negligible in 0.005 M $CDCl_3$ solution, monomers are believed to be predominant at this dilute concentration. For higher concentration, the IR spectra reflect a mixture of monomers and dimers. Finally, at the highest concentration, 0.2 M, the IR spectrum is dominated by the dimeric form of **1**.

The concentration dependence of the IR spectrum of $CDCl_3$ solution of **1** in the C═O stretching region (see Figure 1b) provides additional information regarding the dimerization of **1**. The intensity of the band at 1789 cm^{-1} is independent of the concentration and can be assigned unambiguously to the C═O stretching vibration of the ketone groups. On the other hand, the intensity of the band at 1726 cm^{-1} increases with increasing concentration, while the bands at 1752 and 1778 cm^{-1} disappear. These three bands can be assigned to the C═O stretching vibration of the COOH groups of monomers (1752 and 1778 cm^{-1}) and dimers (1726 cm^{-1}). The others bands observed in the mid-IR spectral region are independent of the concentration, except the bands at 1366 and 1305 cm^{-1}, whose intensities decrease and increase, respectively, with increasing concentration. These two bands are assigned to the COH bending vibration of monomers (1366 cm^{-1}) and dimers (1305 cm^{-1}). Finally, the band at 1098 cm^{-1} appears to be affected by the solution concentration. The frequencies observed in the experimental IR spectra and calculated at the B3PW91/cc-pVTZ level (vide infra) for the conformer **1c** as well as their assignments based on internal coordinates are reported in Table 1 of the Supporting Information.

The VCD spectra of **1** in $CDCl_3$ solution in the OH/CH stretching region and in the mid-IR spectral region are shown in Figure 2a and b, respectively. Figure 2a reveals VCD bands associated with methyl and methylene groups of the camphanic cycle. The sign of the bands and their intensities are similar to those of (*R*)-camphor.[14] A negative band exhibiting a very weak intensity ($\Delta\epsilon \approx 0.0006$) is also observed at 3490 cm^{-1} associated with the OH stretching vibration of "free" COOH groups. Figure 2b shows that, over the spectral range studied, the VCD intensities of **1** vary widely. The VCD bands related to the C═O stretching vibrations are not easily measurable, whereas large VCD intensities are obtained in the 1400−1050 cm^{-1} spectral range. Moreover, the VCD spectrum of dilute (0.005 M) $CDCl_3$ solution presents significant spectral differences from those recorded at higher concentrations. Indeed, this spectrum is essentially dominated by the large intensity of the positive VCD band at 1098 cm^{-1} related to the monomeric form of **1**. This band disappears on the VCD spectra recorded for higher concentrations. A similar conclusion can be drawn for the small bisignate feature observed at 1370 cm^{-1} in the VCD spectrum of the dilute solution.

The IR and VCD spectra of a 0.050 M $CDCl_3$ solution of **2** in the mid-IR spectral region are also reported in Figure 1 of the Supporting Information.

Conformational Analysis of 1 and 2. The analysis of the IR and VCD spectra of **1** and **2** begins with the prediction of its optimized geometries. The conformational flexibility of **1** and **2** arises from the rotation around the single bond C_1C_6. The initial dihedral angle of the O_{12}═C_6–C_1–O_{13} segment of **1** (**2**) is chosen to be 0° and 180°, yielding two conformers **1a** (**2a**) and **1b** (**2b**), respectively (see Chart 1). For the camphanic acid, rotation around the single bond C_6O_{14} is also possible, leading to a third conformer (**1c**) stabilized by intramolecular hydrogen-bonding between the hydroxyl and lactone groups. The dimer of camphanic acid is formed by intermolecular hydrogen-bonding between two COOH groups of two molecules of **1**. Because only the conformers **1a** and **1b** can form intermolecular hydrogen-bonding, four dimers are possible, **1aa**, **1bb**, **1ab**, and **1ba**. The two last conformers **1ab** and **1ba** are equivalent and equi-energetic. The geometries of all previously described conformers were optimized at the B3PW91/cc-pVTZ level. Harmonic vibrational frequencies have been calculated at the same level to confirm that all structures are stable conformations and to enable free energies to be calculated. The converged O_{12}═C_6−C_1−O_{13} dihedral angles, electronic and Gibbs energies, and populations determined from Gibbs energies are listed in Table 1. The optimized energies of **1** and **2** are dependent on the position of the COOH and COCl groups with respect to the camphanic cycle. When the carbonyl group (O_{12}═C_6) adopts a trans orientation with respect to the C_1−O_{13} bond,

TABLE 1: Conformations and Energies of Monomers and Dimers of (1*S*,3*R*)-Camphanic Acid and of (1*S*,3*R*)-Camphanic Chloride

	converged dihedral angles[a]		energy[b]		ΔG_c	population[d]
conformer	D_1 (deg)	D_2 (deg)	electronic	Gibbs	(kJ/mol)	(%)
1a	−15.9	177.9	−690.406441	−690.213819	6.92	4.2
1b	169.0	−178.7	−690.408222	−690.215533	2.42	25.9
1c	176.2	2.1	−690.409932	−690.216456	0	69.9
1aa	−15.8	177.8	−1380.840576	−1380.434203	1.92	14.0
1bb	165.7	−178.8	−1380.841475	−1380.434730	0.54	24.6
1ab	−17.1	177.5	−1380.840649	−1380.434936	0	61.4[e]
	164.1	−177.6				
2a	−14.5		−1074.745243	−1074.567534	5.31	10.2
2b	167.9		−1074.746962	−1074.569557	0	89.8

[a] Dihedral angles: D_1, $O_{12}=C_6-C_1-O_{13}$; D_2, $H-O_{14}-C_6-C_1$. [b] In hartrees. [c] Relative Gibbs energy difference. [d] Population based on Gibbs energies. [e] Statistical weighting factor of 2 accounting for the equivalent conformers **1ab** and **1ba**.

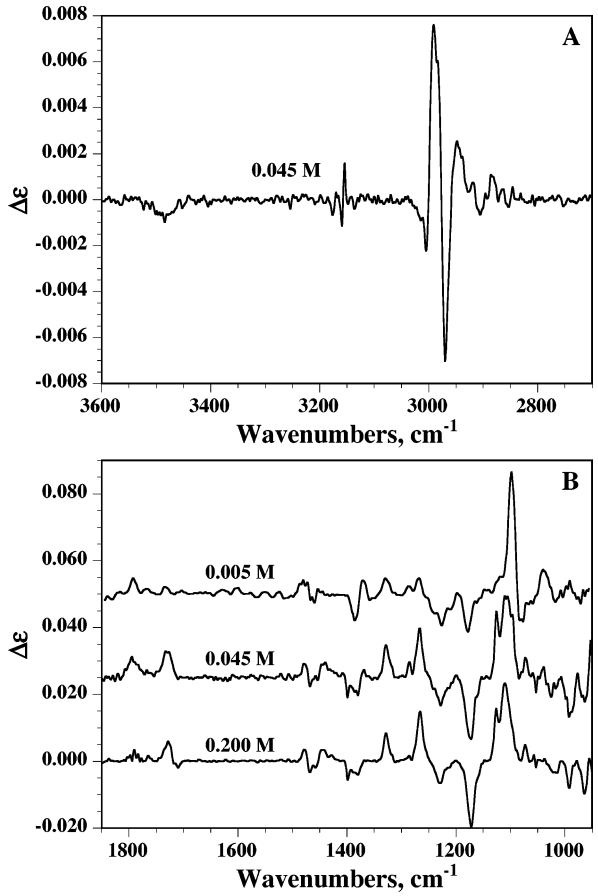

Figure 2. (A) VCD spectrum of **1** in $CDCl_3$ solution in the OH/CH stretching region. (B) Concentration dependence of the VCD spectra of **1** in $CDCl_3$ solution in the mid-IR spectral region. The VCD spectrum of 0.005 M solution has been smoothed to reduce the spectral noise.

the conformers (**1b** and **2b**) have lower energies than those calculated for a cis orientation (**1a** and **2a**). Moreover, for the camphanic acid, the formation of an intramolecular hydrogen-bond between the hydroxyl and lactone groups leads to the most stable conformer (**1c**) by 2.42 kJ/mol. The O···H and O···O intramolecular hydrogen-bonding distances in **1c** are 1.96 and 2.59 Å, while the O···H−O angle is 120.6°. The optimized energies of the dimer form of **1** are less sensitive to the position of the COOH group with respect to the camphanic cycle. Nevertheless, although conformers **1ab** and **1bb** differ in energy by 0.54 kJ/mol, the statistical weighting factor of 2 for dimer **1ab** yields relative populations of 61.4% **1ab**, 24.6% **1bb**, and 14% **1aa**. The O···H and O···O intermolecular hydrogen-bonding distances in **1ab** are 1.60 and 2.62 Å, while the O···H−O angle is 178.7°. It is important to note that these calculations have been achieved for isolated molecules in the gas phase, whereas experiments were performed in $CDCl_3$ solutions. It is possible that solvation effects modify the calculated conformational equilibrium in particular for the monomeric forms of camphanic acid and camphanic chloride.

Calculated IR and VCD Spectra of the Monomeric Form of 1. The IR and VCD spectra calculated at the B3PW91/cc-pVTZ level for individual conformers (**1a**, **1b**, and **1c**) and the final population-weighted spectra are shown in Figures 3 and 4, respectively, and compared to the corresponding experimental IR and VCD spectra of **1** in dilute (0.005 M) $CDCl_3$ solution. The experimental IR and VCD spectra in dilute solution have been chosen for comparison as they are less affected by dimerization of **1**. Indeed, in dilute solution, the intermolecular hydrogen-bonding between COOH groups becomes negligible, allowing a better comparison of experimental and predicted spectra of the monomeric form of **1**.

Figure 3 shows that the predicted absorption spectrum is in relatively good agreement with the experimental spectrum of **1**, except for the bands associated with OH stretching and COH bending vibrations. Indeed, the OH stretching frequencies of conformer **1a**, **1b**, and **1c** are predicted at higher wavenumbers than that observed at 3494 cm^{-1} in the experimental spectrum, and the COH bending intensity at 1366 cm^{-1} is overestimated. However, the OH stretching frequency calculated for conformer **1c** is significantly lower than those calculated for conformers **1a** and **1b**, due to the intramolecular hydrogen-bonding between hydroxyl and lactone groups. In the mid-IR region, the C═O stretching vibration of the ketone group is calculated at nearly the same frequency for the three conformers, whereas two distinct frequencies are calculated for the C═O stretching vibration of the carbonyl group. Consequently, the predicted absorption spectrum exhibits three bands in the C═O stretching region as described above (the fourth band observed at 1726 cm^{-1}, with very low intensity in the experimental spectrum, is assigned to the C═O stretching vibration of dimers).

Figure 4 shows that the predicted VCD spectrum reproduces fairly well the intensity and the sign of the bands observed in the experimental spectrum, allowing the definitive determination of the configuration and the conformation of the molecule in its monomeric form. The VCD spectra calculated for individual conformer in the CH stretching region are not dependent on the conformation of **1** and reproduce very well the experimental spectrum (see Figure 4a). Conversely, the sign and the intensity of the VCD band associated with the OH stretching vibration depend on the conformation of the molecule. The negative sign predicted for the population-weighted spectrum is in agreement

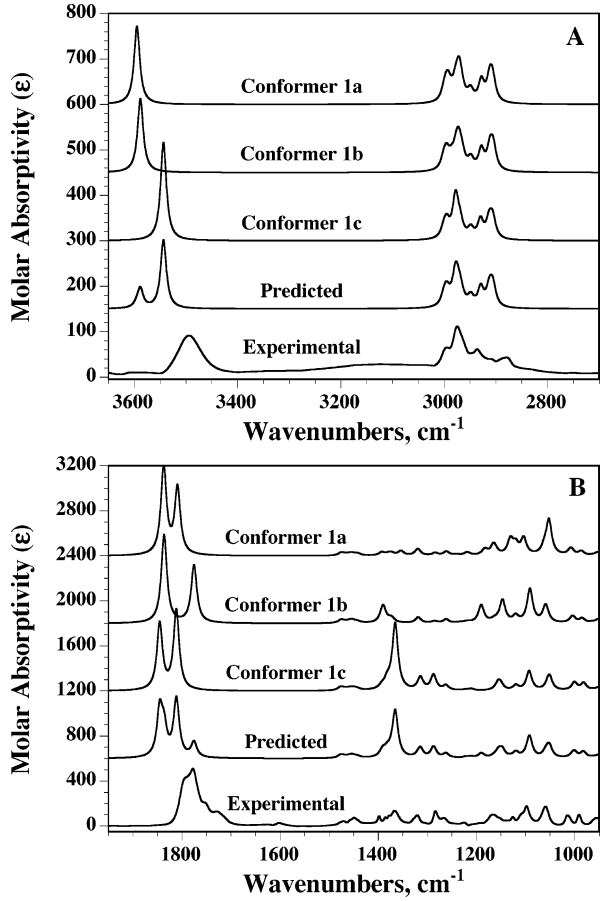

Figure 3. Comparison of the experimental absorption spectrum of **1** in 0.005 M $CDCl_3$ solution with individual conformer spectra and predicted (population-weighted) absorption spectrum calculated using the B3PW91/cc-pVTZ level in (A) the 3650−2700 cm^{-1} and (B) the 1950−950 cm^{-1} regions. The DFT spectra were simulated with Lorentzian band shapes (7 cm^{-1} half-width), and the frequencies were scaled by 0.954 and 0.978 in the 3650−2700 cm^{-1} and 1950−950 cm^{-1} regions, respectively.

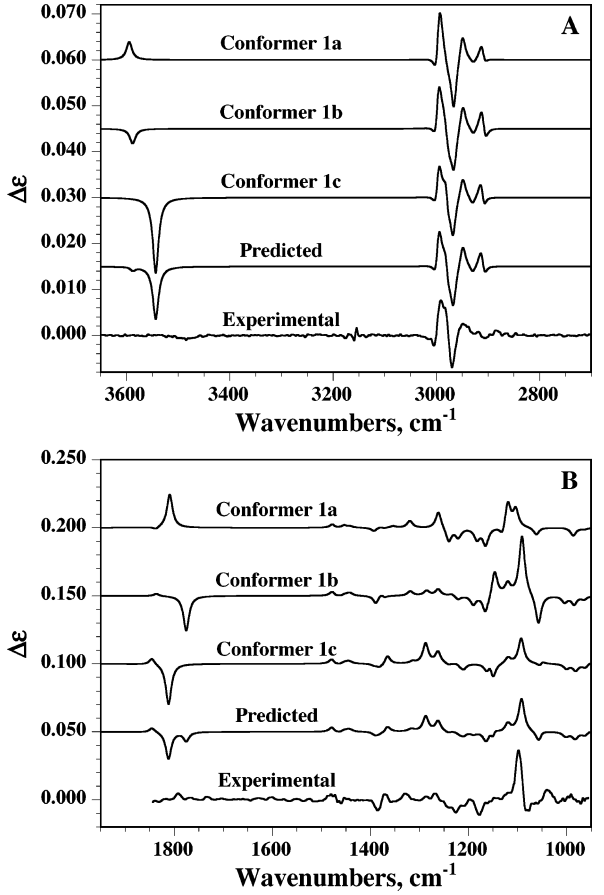

Figure 4. Comparison of the experimental VCD spectrum of **1** in $CDCl_3$ solution with individual conformer spectra and predicted (population-weighted) VCD spectrum calculated using the B3PW91/cc-pVTZ level in (A) the 3650−2700 cm^{-1} and (B) the 1950−950 cm^{-1} regions. The DFT spectra were simulated with Lorentzian band shapes (7 cm^{-1} half-width), and the frequencies were scaled by 0.954 and 0.978 in the 3650−2700 cm^{-1} and 1950−950 cm^{-1} regions, respectively.

with that observed in the experimental spectrum, but the intensity of the VCD band is not correct. This discrepancy can be attributed to the half-width of the band being larger in the experimental spectrum (25 cm^{-1}) than in the calculated one (7 cm^{-1}). In the mid-IR region (Figure 4b), the experimental and predicted VCD spectra match fairly well, except for the C═O stretching vibration of the carbonyl groups. Indeed, two negative bands are predicted, whereas no significant contributions are observed in the experimental spectrum. On the other hand, the weak positive contribution observed for the C═O stretching vibration of the ketone groups is well predicted. More interesting, the strong VCD contribution observed for the band at 1098 cm^{-1}, unambiguously related to the monomeric form of **1**, is well predicted. These results show that the absolute conformation of the monomeric form of **1** can be determined from the VCD spectrum of dilute $CDCl_3$ solution, in which intermolecularly hydrogen-bonded dimers are negligible. Moreover, we have demonstrated that VCD experiments for dilute solution are possible even if the signal-to-noise ratio of the VCD spectra is dramatically reduced by the interference from solvent absorption.

Calculated IR and VCD Spectra of the Dimeric Form of 1. Figure 5a and b shows the IR and VCD spectra calculated at the B3PW91/cc-pVTZ level for the three dimer conformers (**1aa**, **1bb**, and **1ab**), the final population-weighted spectrum, and the corresponding experimental spectra in the mid-IR region of **1** in 0.2 M $CDCl_3$ solution. As previously mentioned in the literature[2,7,8] and observed in Figures 1 and 2, dramatic changes are observed in both the IR and the VCD spectra in going from monomer to dimer. In particular, the VCD spectra of dimer conformers show a Lorentzian derivative shape for the C═O stretching vibrations. These VCD couplets, for which the intensity and the sign depend on the dimer conformer, arise from the coupling of the two carbonyl dipoles (in- and out-of-phase modes) and can be interpreted using the degenerate coupled oscillator model.[15,16] Moreover, the intensities of the VCD bands at 1328, 1266, and 1172 cm^{-1} are observed to be larger for the dimer than for the monomer. Finally, the intense band observed at 1098 cm^{-1} in the VCD spectrum of monomer disappears at higher concentration and is replaced by two positive bands at 1126 and 1110 cm^{-1}. Most of the spectral modifications observed in the VCD spectrum of the dimer form of **1** are well reproduced in the calculated VCD spectra of dimer conformers (Figure 5b). On the other hand, the predicted (population-weighted) IR and VCD spectra are in excellent agreement with the corresponding experimental spectra, thus confirming that the dimer conformer **1ab** is the most abundant species in 0.2 M $CDCl_3$ solution. A better agreement between predicted and experimental spectra is found for the dimer as solvent effects are less pronounced, particularly for the vibrations associated to the COOH group.

Calculated IR and VCD Spectra of 2. The IR and VCD spectra calculated at the B3PW91/cc-pVTZ level for individual

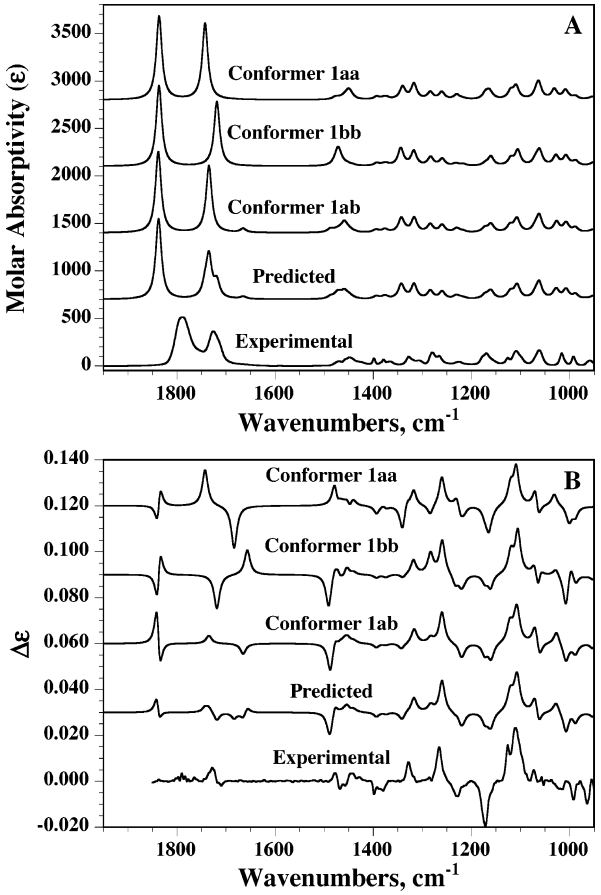

Figure 5. (A) Comparison of the experimental IR spectrum of **1** in 0.2 M $CDCl_3$ solution with individual dimer conformer spectra and predicted (population-weighted) IR spectrum calculated using the B3PW91/cc-pVTZ level. (B) Comparison of the experimental VCD spectrum of **1** in 0.2 M $CDCl_3$ solution with individual dimer conformer spectra and predicted (population-weighted) VCD spectrum of dimer calculated using the B3PW91/cc-pVTZ level. The DFT spectra were simulated with Lorentzian band shapes (7 cm^{-1} half-width), and the frequencies were scaled by 0.978.

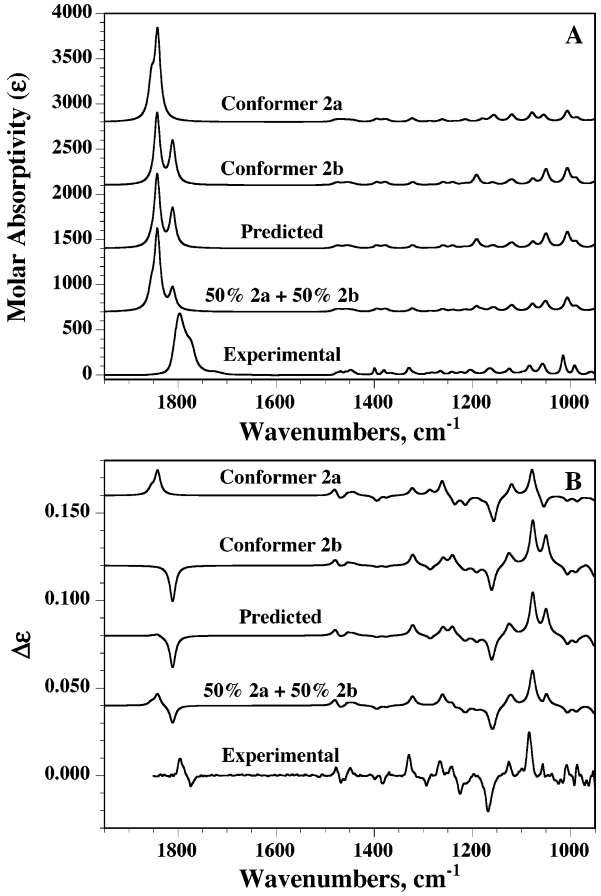

Figure 6. (A) Comparison of the experimental IR spectrum of **2** in 0.050 M $CDCl_3$ solution with individual conformer spectra, predicted (population-weighted) IR spectrum, and half-sum of spectra of conformers **2a** and **2b** calculated using the B3PW91/cc-pVTZ level. (B) Comparison of the experimental VCD spectrum of **2** in 0.050 M $CDCl_3$ solution with individual conformer spectra, predicted (population-weighted) VCD spectrum, and half-sum of spectra of conformers **2a** and **2b** calculated using the B3PW91/cc-pVTZ level. The DFT spectra were simulated with Lorentzian band shapes (7 cm^{-1} half-width), and the frequencies were scaled by 0.978.

conformers (**2a** and **2b**) and the final population-weighted spectra are shown in Figure 6 and compared to the corresponding experimental IR and VCD spectra of **2** in 0.050 M $CDCl_3$ solution. As observed for the camphanic acid, the VCD spectra of individual conformers are significantly different, in particular in the C═O stretching region. When the carbonyl group (O_{12}═C_6) adopts a trans orientation with respect to the C_1-O_{13} bond (conformers **1b**, **1c**, and **2b**), a negative contribution is calculated for the VCD band associated with the C═O stretching vibration of the COX group (X = OH or Cl), whereas a positive contribution is calculated for a cis orientation (conformers **1a** and **2a**).

The predicted VCD spectrum for **2** does not match well with the experimental VCD spectrum. The most notable difference between experimental and predicted VCD spectra is seen in the C═O stretching region and for the band located at 1056 cm^{-1}. A better agreement has been found considering the half-sum of the calculated VCD spectra of the two conformers (see Figure 6b). The relative population of **2a** and **2b** may have been incorrectly determined previously, because the molecular interactions between the solvent ($CDCl_3$) and the camphanic chloride molecule have not been taken into account in the calculations. Indeed, the preferential interaction between the choride and lactone groups stabilizing the conformer **2b** should be attenuated in the presence of $CDCl_3$ molecules. Moreover, the relative Gibbs energy difference (ΔG) decreases significantly when the solvation effect on the optimized geometries was introduced phenomenologically through a continuum model calculation (Onsager model).

4. Conclusion

This paper shows that modeling of vibrational circular dichroism spectra using density functional theory can be successfully performed to determine the absolute configurations and conformations of chiral carboxylic acids, even if these molecules associate through hydrogen-bonding. This methodology consisting of comparison of experimental and calculated spectra of one enantiomer with a given conformation was applied to camphanic acid and camphanic chloride in $CDCl_3$ solution. The absolute conformation of the monomeric form of camphanic acid has been determined from a dilute (0.005 M) solution, whereas a more concentrated (0.2 M) solution has been used to determine the absolute conformation of its dimeric form. The population-weighted predicted IR and VCD spectra for monomeric and dimeric camphanic acid were found to be in good agreement with the corresponding experimental spectra. In the dilute solution, the conformer with intramolecular hydrogen-bonding between the hydroxyl and lactone groups was of lowest energy and represents 70% of the different monomer

conformers at room temperature, whereas in concentrated solution the dimer formed by intermolecular hydrogen-bonding of carboxyl groups of the two distinct monomer conformations was stabilized. On the other hand, the experimental IR and VCD spectra of camphanic chloride did not match well with the population-weighted spectra predicted from DFT calculations. This may be due to the intermolecular interactions with the solvent, which were not taken into account in our calculations.

Acknowledgment. We are indebted to the CNRS (Chemistry Department) and to Région Aquitaine for financial support in FTIR and optical equipment. We also gratefully acknowledge the SIMOA of the ENSCPB (Université Bordeaux I) for allocating computing time and providing facilities.

Supporting Information Available: Experimental frequencies, B3PW91/cc-pVTZ unscaled frequencies, and assignment of the normal modes of **1c** conformer of (−)-(1*S*,3*R*)-camphanic acid. Experimental IR and VCD spectra of (−)-(1*S*,3*R*)-camphanic chloride in the 1850−950 cm^{-1} spectral range. This material is available free of charge via the Internet at http://pubs.acs.org.

References and Notes

(1) Nafie, L. A.; Dukor, R. K.; Freedman, T. B. In *Handbook of Vibrational Spectroscopy*; Chalmers, J. M., Griffiths, P. R., Eds.; John Wiley & Sons: Chichester, 2002; Vol. 1, pp 731−744.

(2) Freedman, T. B.; Cao, X.; Dukor, R. K.; Nafie, L. A. *Chirality* **2003**, *15*, 743−758 and references therein.

(3) Stephens, P. J.; Delvin, F. J. *Chirality* **2000**, *12*, 172−179.

(4) Chincilla, R.; Najera, C.; Yus, M.; Heumann, A. *Tetrahedron: Asymmetry* **1990**, *1*, 851−854.

(5) Naegeli, P.; Wirz-Habersack, Y. *Tetrahedron: Asymmetry* **1992**, *3*, 221−222.

(6) Brotin, T.; Barbe, R.; Darzac, M.; Dutasta, J. P. *Chem.-Eur. J.* **2003**, *9*, 5784−8792.

(7) He, J.; Polavarapu, P. L. *J. Chem. Theory Comput.* **2005**, *1*, 506−514.

(8) Urbanova, M.; Setnicka, V.; Delvin, F. J.; Stephens, P. J. *J. Am. Chem. Soc.* **2005**, *127*, 6700−6711.

(9) Buffeteau, T.; Lagugné-Labarthet, F.; Sourrisseau, C. *Appl. Spectrosc.* **2005**, *59*, 732−745.

(10) Nafie, L. A.; Vidrine, D. W. In *Fourier Transform Infrared Spectroscopy*; Ferraro, J. R., Basile, L. J., Eds.; Academic Press: New York, 1982; Vol. 3, pp 83−123.

(11) Frisch, M. J.; Trucks, G. W.; Schlegel, H. B.; Scuseria, G. E.; Robb, M. A.; Cheeseman, J. R.; Montgomery, J. A., Jr.; Vreven, T.; Kudin, K. N.; Burant, J. C.; Millam, J. M.; Iyengar, S. S.; Tomasi, J.; Barone, V.; Mennucci, B.; Cossi, M.; Scalmani, G.; Rega, N.; Petersson, G. A.; Nakatsuji, H.; Hada, M.; Ehara, M.; Toyota, K.; Fukuda, R.; Hasegawa, J.; Ishida, M.; Nakajima, T.; Honda, Y.; Kitao, O.; Nakai, H.; Klene, M.; Li, X.; Knox, J. E.; Hratchian, H. P.; Cross, J. B.; Adamo, C.; Jaramillo, J.; Gomperts, R.; Stratmann, R. E.; Yazyev, O.; Austin, A. J.; Cammi, R.; Pomelli, C.; Ochterski, J. W.; Ayala, P. Y.; Morokuma, K.; Voth, G. A.; Salvador, P.; Dannenberg, J. J.; Zakrzewski, V. G.; Dapprich, S.; Daniels, A. D.; Strain, M. C.; Farkas, O.; Malick, D. K.; Rabuck, A. D.; Raghavachari, K.; Foresman, J. B.; Ortiz, J. V.; Cui, Q.; Baboul, A. G.; Clifford, S.; Cioslowski, J.; Stefanov, B. B.; Liu, G.; Liashenko, A.; Piskorz, P.; Komaromi, I.; Martin, D. J.; Fox, T.; Keith, M. A.; Al-Laham, C. Y.; Peng, A.; Nanayakkara, M.; Challacombe, R. L.; Gill, P. M. W.; Johnson, B.; Chen, W.; Wong, M. W.; Gonzalez, C.; Pople, J. A. *Gaussian 03*, revision B.04; Gaussian, Inc.: Pittsburgh, PA, 2003.

(12) Cheeseman, J. R.; Frisch, M. J.; Delvin, F. J.; Stephens, P. J. *Chem. Phys. Lett*. **1996**, *252*, 211−220.

(13) Novak, A. In *Struct. Bonding 18*; Dunitz, J. D., et al., Eds.; Springer-Verlag: New York, 1974; pp 177−216.

(14) Cao, X.; Shah, R. D.; Dukor, R. K.; Guo, G.; Freedman, T. B.; Nafie, L. A. *Appl. Spectrosc.* **2004**, *58*, 1057−1064.

(15) Holzwarth, G.; Chabay, I. *J. Chem. Phys*. **1972**, *57*, 1632.

(16) Tinoco, I. *Radiat. Res.* **1963**, *20*, 133.